Journal of Volcanology and Geothermal Research 308 (2015) 70–81

Contents lists available at ScienceDirect

Journal of Volcanology and Geothermal Research

journal homepage: www.elsevier.com/locate/jvolgeores

The Carrán–Los Venados volcanic field and its relationship with coeval and nearby polygenetic volcanism in an intra-arc setting

Francisco Bucchi [a,*], Luis E. Lara [a], Francisco Gutiérrez [b]

[a] Servicio Nacional de Geología y Minería, Red Nacional de Vigilancia Volcánica, Santiago, Chile
[b] Departamento de Geología, Universidad de Chile, Santiago, Chile/ Centro de Excelencia en Geotermia de los Andes (CEGA)/ Advanced Mining Technology Center (AMTC)

ARTICLE INFO

Article history:
Received 11 May 2015
Accepted 7 October 2015
Available online 22 October 2015

Keywords:
Carrán–Los Venados
Monogenetic volcanic field
Monogenetic and polygenetic volcanism coexistence

ABSTRACT

Understanding the relationship between monogenetic and polygenetic volcanism has been a long-standing goal in volcanology, especially in cases where these two styles of volcanism are coeval and geographically adjacent. We studied the Carrán–Los Venados (CLV) volcanic field and made comparisons with published data on CLV's polygenetic neighbor Puyehue–Cordón Caulle (PCC) in the Southern Andean arc, using quantitative tools and recent numerical simulations of magma reservoir formation. CLV is a basaltic to basaltic andesitic volcanic field composed of 65 post-glacial scoria cones and maars and a 1-km-high Pleistocene stratovolcano, whereas PCC is a basaltic to rhyolitic composite volcano. Our results point to three main differences between CLV and PCC: (1) the CLV magmas differentiate at low-crustal reservoirs, followed by rapid ascent to the surface, while the PCC magmas stagnate and differentiate in lower- and upper-crustal reservoirs; (2) CLV is elongated in the NE direction while PCC is elongated in the NW direction. Under the current stress field (N60°E σ_{Hmax}), these two volcanic alignments correspond, respectively, to local extensional and compressive deformation zones within the arc; and (3), the post-glacial CLV magma flux was estimated to be 3.1 ± 1.0 km^3/ky, which is similar to the average magma flux estimated for PCC; however, the PCC magma flux is estimated at approximately twice this value during peak eruptive periods (5.5 ± 1.1 km^3/ky). Based on numerical simulations, CLV is in a limit situation to create and sustain a mush-type upper-crustal reservoir containing highly crystalline magma, which is however not eruptible. The PCC volcanic system would have been able to create a stable reservoir containing eruptible silicic magma during periods of peak magma flux. We postulate that monogenetic volcanism occurs at CLV due to both low magma flux and an extensional/transtensional regime that favors rapid magma rise without storage and differentiation in stable upper-crustal reservoirs. However, the CLV system seems to be at an inflection point, and could become polygenetic if magma flux increases. For PCC, high magma flux during some periods together with compressive deformation would have led to the construction of one or several stable upper-crustal magma reservoirs, with subsequent silicic volcanism and construction of central conduits for magma extrusion, resulting in polygenetic volcanism with evolved compositions. In this model, monogenetic volcanic systems can become polygenetic despite extensional regime if magma flux increases sufficiently to create and sustain a stable upper-crustal magma reservoir.

1. Introduction

Monogenetic and polygenetic volcanism are the two classic and opposite styles of volcanism (Nakamura, 1977; Takada, 1994; Martin et al., 2003; Cañón-Tapia and Walker, 2004), each associated with different sub-volcanic structures: monogenetic volcanic fields lack stable upper-crustal magma reservoirs, while polygenetic volcanoes have one or several stable upper-crustal reservoirs (Fedotov, 1981; Takada, 1994; López-Escobar et al., 1995; Cañón-Tapia and Walker, 2004; Lara et al., 2006a). Monogenetic volcanism is characterized by the formation of a volcanic vent through one single eruption, most commonly basaltic (*e.g.* Nakamura, 1977; Németh, 2010). However, a wide range of chemical compositions occur in volcanic fields, both in arc (*e.g.* Chichinautzin) (Straub et al., 2011) and in intraplate settings (*e.g.* Jeju) (Brenna et al., 2010). Monogenetic volcanic activity tends to form volcanic fields, themselves formed by clusters of vents (Condit and Connor, 1996; Le Corvec et al., 2013b). Monogenetic eruptions are generally, but not exclusively, small-volume (*e.g.* Connor et al., 2000, 2012). Finally, monogenetic volcanic fields tend to have low average magma output rates (Fedotov, 1981; Walker, 1993). Although polygenetic volcanism is as varied as monogenetic volcanism, it is usually characterized by the presence of relatively more differentiated andesitic to rhyolitic magmas, a central conduit that channels the magma in most eruptions, and high average magma output rates.

* Corresponding author at: Red Nacional de Vigilancia Volcánica, Av. Santa María 0104, Santiago, Chile. Tel.: +56 9 90793948.
E-mail address: francisco.bucchi@gmail.com (F. Bucchi).

http://dx.doi.org/10.1016/j.jvolgeores.2015.10.013
0377-0273/

Coexistence in time and space of monogenetic and polygenetic volcanoes having such contrasting characteristics is an intriguing topic in volcanology. Nakamura (1977) noted that monogenetic volcanism is favored in extensional tectonics, and other authors have proposed that the style of volcanism may be determined by the magma supply rate (Fedotov, 1981; Hildreth, 1981; Takada, 1994; Cañón-Tapia and Walker, 2004), the magma extrusion/intrusion rate (Hildreth, 1981) and/or crustal tectonics (Takada, 1994; Cañón-Tapia and Walker, 2004; Valentine and Perry, 2007). Nowadays, more precise quantitative studies on monogenetic and polygenetic volcanism have become possible, through the use of a number of tools such as numerical simulations of upper-crustal magma reservoir formation (*e.g.* Annen, 2009; Gelman et al., 2013; Menand et al., 2015), statistical analysis of vent distribution within volcanic fields (*e.g.* Hammer, 2009; Connor et al., 2012; Runge et al. 2014), and extensive geochronological and geochemical characterization of volcanoes in general (*e.g.* Singer et al., 2008). Thus, it is possible to re-evaluate these controlling factors and understand whether distributed venting is a permanent condition or a step toward central systems in arc volcanoes.

In this article, we study the relationship between monogenetic and polygenetic volcanism in a strike-slip intra-arc setting. The case study is the Carrán–Los Venados (CLV) volcanic field and its polygenetic neighbor Puyehue–Cordón Caulle (PCC) (Fig. 1), for which a possible connection at the mantle source and/or lower-crust has been suggested (Lara et al., 2006a). For PCC, compositions, time–volume relationships and ages are available (*e.g.* Lara et al., 2004; Sepúlveda et al., 2005; Singer et al., 2008), but this is not the case for CLV, and this study aims to expand existing knowledge about CLV.

The evidence in this article is presented as follows: (1) spatial distribution analyses were performed in order to determine the clustering and alignments of minor eruptive centers (MEC) within CLV. This type of study provides abundant information about the plumbing system of monogenetic volcanic fields, because the distribution of volcanoes within these fields is thought to be the result of a competition between deep magmatic processes and shallow structural control on magma rise (Tibaldi, 1995; Condit and Connor, 1996; Kiyosugi et al., 2010; Németh, 2010; Le Corvec et al., 2013b; Tibaldi, 2015); (2) the source of CLV magmas and their differentiation processes were characterized using petrography and geochemistry; and (3) CLV time–volume relationships were estimated and used to evaluate the formation of upper-crustal magma reservoirs, using a model of incrementally formed reservoir that takes into account basaltic and silicic compositions (Gelman et al., 2013). In this model, potentially eruptible magma is available in upper-crustal reservoirs only if it has accumulated at rates that exceed a certain threshold. Finally, we discuss the hypothesis of monogenetic volcanic fields as precursors of polygenetic volcanism (López-Escobar and Moreno, 1994).

2. Geological setting

The CLV volcanic field is located in the Central Southern Volcanic Zone (CSVZ, 37°–42°S) (López-Escobar et al., 1995), which is characterized by a *ca.* 35-km-thick crust (Hildreth and Moorbath, 1988) and the oblique convergence of the Nazca and South America plates (Fig. 1). Volcanism in the CSVZ is spatially related to the Liquiñe Ofqui Fault-Zone (LOFZ), which is a 1200 km-long, major long-lived intra-arc fault

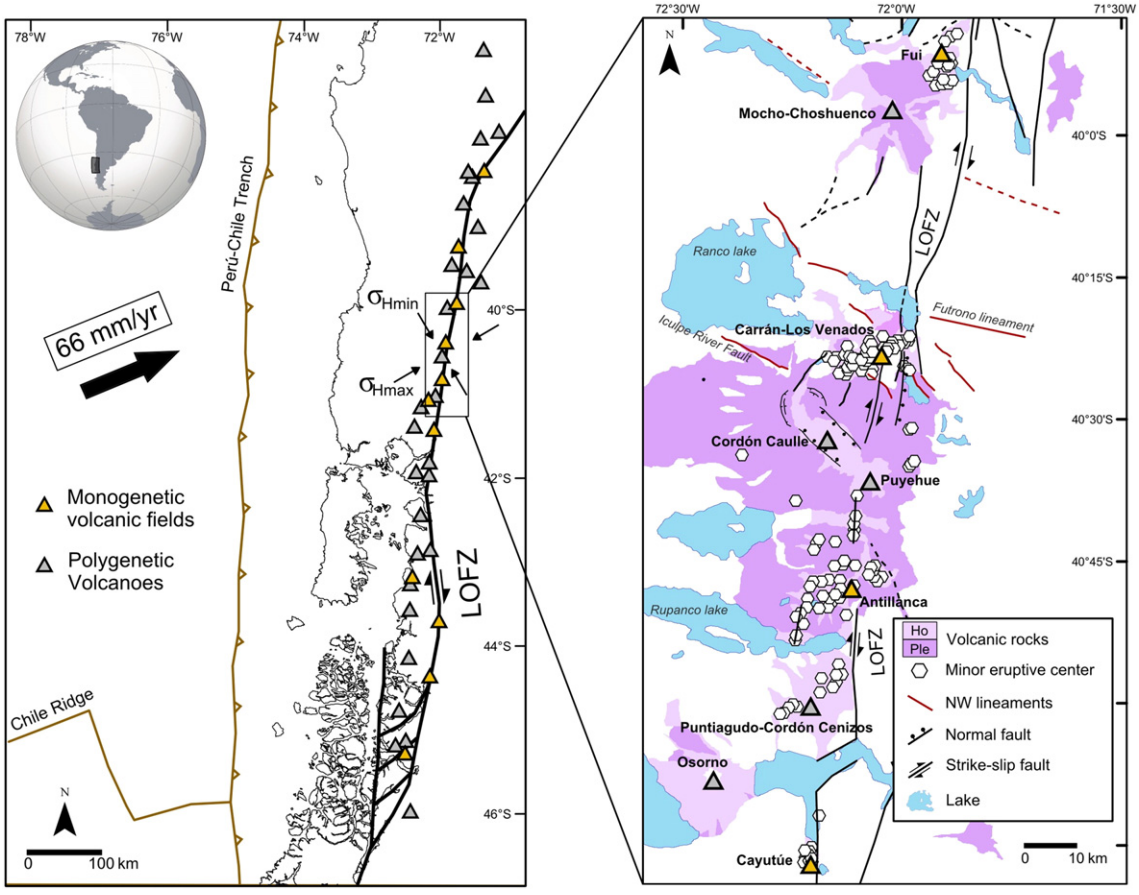

Fig. 1. (a) Tectonic setting of the Andean Southern Volcanic Zone (33–46°S). Oblique convergence induces dextral-shearing in the intra-arc zone between 38 and 46°S, where polygenetic and monogenetic volcanic fields alternate. Quaternary stress field in the intra-arc zone shows a N60°E-trending maximum horizontal stress, inferred from shallow earthquakes and stress tensors (Lavenu and Cembrano, 1999; Rosenau et al., 2006) and coincides with plate convergence vector. (b) Sketch map showing distribution of volcanism in Carrán–Los Venados and Puyehue–Cordón Caulle area. Faults were compiled from Campos et al. (1998); Lara et al. (2006a); and Rosenau et al. (2006).

system (Cembrano et al., 1996; Rosenau et al., 2006). The LOFZ accommodates deformation along the intra-arc domain by dextral strike-slip shearing along the NNE-striking master fault in a bulk transpressive regime (Lavenu and Cembrano, 1999; Rosenau et al., 2006; Cembrano and Lara, 2009). Fault-slip data and stress tensors for Pleistocene deformation along the northern portion of the LOFZ consistently show a subhorizontal maximum principal compressive stress (σ_{Hmax}) trending N60°E (Lavenu and Cembrano, 1999; Rosenau et al., 2006), which can also be inferred from some focal mechanisms of crustal earthquakes (Barrientos and Acevedo, 1992), and is coincident with the angle of plate convergence (Angermann et al., 1999).

In addition to LOFZ, NW-striking fault zones have been documented in the CSVZ and in the CLV area (Lara et al., 2006a). These faults have been interpreted as crustal-scale weaknesses associated with pre-Andean faults, and are thought to have reactivated under the prevailing stress field as sinistral-reverse strike-slip faults during arc development (Lara et al., 2006a,b; Rosenau et al., 2006; Glodny et al., 2008; Lange et al., 2008). These faults are capable of reactivation during co- and post-seismic relaxation (Lara et al., 2004).

2.1. The Carrán–Los Venados volcanic field

The CLV volcanic field (40.35°S/72.07°W) is a cluster of 65 scoria cones and maars, and the 1-km-high Los Guindos stratovolcano, all of them distributed in ~160 km^2 (Fig. 2). Eruptive styles are strombolian and phreatomagmatic, the latter being more frequently close to the LOFZ master faults. The MECs in CLV form a N60–70°E-trending 4-km wide and 17-km long corridor. The Los Guindos stratovolcano and a group of 3 scoria cones called Medialuna are distinguished in CLV as peripheral centers on the basis of geochemical data, and because they are not located exactly within the main group of MECs (Moreno, 1977; Rodríguez, 1999). The basement of the area largely comprises Paleozoic to Miocene arc intrusive rocks, with a few outcrops of Oligocene–Miocene sedimentary strata in the western part of the field (Campos et al., 1998).

The onset of volcanism at CLV is marked by the oldest Los Guindos unit, and is assigned a Mid-to-Late Pleistocene age due to the evidence of glacial erosion in lavas (Fig. 2) (Campos et al., 1998). All subsequent units have been assigned a post-glacial age (<13.9 ka) because they lack glacial erosion (Campos et al., 1998). This age is supported by six ^{14}C dates made in this study (Table 1). These young units include the upper units of Los Guindos (Holocene lavas and pyroclastics, in Fig. 2), the 'basal lavas', and the overlying pyroclastic and effusive products from the scoria cones and maars (Fig. 2). The 'basal lavas' are extensive lava flows that fill the Riñinahue and Nilahue river valleys. Their emission centers are unknown, but are thought to be now-covered eruptive fissures or vents partially destroyed by subsequent eruptive episodes.

CLV had three eruptions during the 20th century: in 1907, 1955 and 1979. The 1907 eruption had a first phreatomagmatic phase, which produced the Riñinahue maar, followed by an effusive phase that filled the maar with lava. The 1955 eruption was also phreatomagmatic, forming the Carrán maar with steep walls, which are well preserved to date. The third eruption, in 1979, was strombolian and formed the Mirador scoria cone, with a total output volume of ~0.01 km^3 (López-Escobar and Moreno, 1981).

Three structural systems are present in the study area (Fig. 2). The most important is the Liquiñe–Ofqui Fault Zone (LOFZ), which is represented here by NNE lineaments. The best-defined of these lineaments is the Contrafuerte river valley, where two eroded scarps are recognizable on Quaternary rocks. Up to 800 m of vertical separation is observed on the eastern hanging wall block. Further East, the normal Huishue fault runs parallel to the main trace of the LOFZ and shows up to 300 m of vertical separation between the western hanging wall block (Miocene granites) and the eastern footwall (Lara et al., 2006a). Further East, the Cullao normal fault parallels the Huishue fault. The trace of this fault extends to the north of Maihue Lake and merges with the trace of the dextral strike-slip LOFZ, which has its morphological expression in the Maqueo, Fiuko and Pillanleufú river valleys (Fig. 2) (Guzmán, 2013).

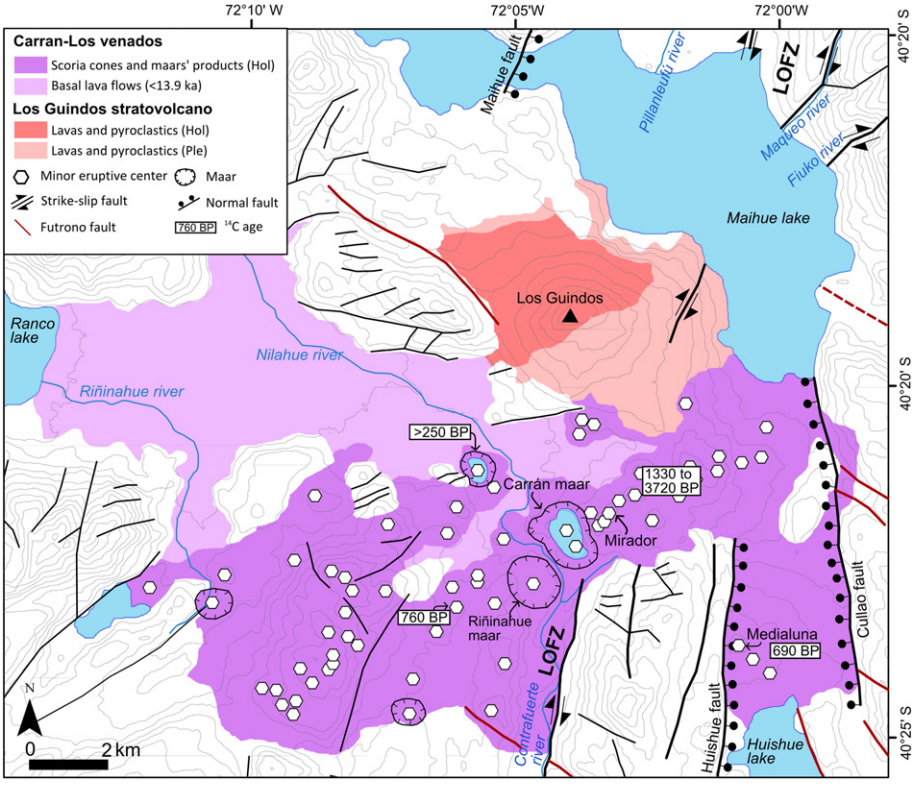

Fig. 2. Simplified geological map of the Carrán–Los Venados area. Geological units are modified from Moreno (1977) and Campos et al. (1998).

Table 1
Results of six ^{14}C datings made in this study.

Latitude	Longitude	Volcano	Dated material	^{14}C age (yrBP ± 2σ)
40°21.231'S	72°5.957'W	Pocura maar	Paleosol over maar's surge deposit	225 ± 75
40°24.262'S	71°59.420'W	Medialuna	Paleosol under Medialuna's lava flow	690 ± 30
40°22.820'S	72°6.635'W	Quilicura centers	Charcoal within the scoria cone	760 ± 30
40°22.030'S	72°1.635'W	Carrán centers	Paleosol in pyroclastic and surge deposits sequence	1330 ± 30
40°22.030'S	72°1.635'W	Carrán centers	Paleosol in pyroclastic and surge deposits sequence	2280 ± 30
40°22.164'S	72°0.666'W	Carrán centers	Paleosol in pyroclastic and surge deposits sequence	3720 ± 30

The second fault system is the NW-striking Futrono fault (Figs. 1 and 2) (Campos et al., 1998). This fault is represented by several well-defined NW lineaments in the granitic basement.

A third ENE system of faults/fractures is inferred from minor morphologic lineaments in basement rocks, whose orientation is shown in the Appendix. The kinematics of this system is not well-constrained, although its orientation is capable of extension under the current stress field. The three 20th century eruptions occurred at the intersection of the LOFZ and the ENE fault/fracture system.

2.2. The Puyehue–Cordón Caulle volcanic complex

Puyehue–Cordón Caulle (PCC) is a 15-km-long by 4-km-wide, NW–SE elongated volcanic complex that includes the Puyehue stratovolcano and the Cordón–Caulle area of fissure volcanism, with an estimated volume of ~140 km^3 (Sepúlveda et al., 2005; Lara et al., 2006b; Singer et al., 2008) (Fig. 1). Volcanism started at approximately 0.5 Ma with dominantly mafic extrusions, then erupting mainly dacitic and rhyolitic (up to 72% SiO_2) magmas in the Holocene (Lara et al., 2006b; Singer et al., 2008). The NW elongation of the volcanic complex is attributed to the long-lived NW-striking Iculpe River fault, believed to serve as a pathway for magma ascent (Lara et al., 2006b). Cordón–Caulle is an elongated volcano-tectonic depression, with normal faults in the edges of a graben (Sepúlveda et al., 2005; Lara et al., 2006b), whereas Puyehue stratovolcano is located at the SE end of Cordón–Caulle, at the intersection of the LOFZ and the Iculpe River fault (Lara et al., 2006b). The silicic volcanism at PCC has been explained in terms of the orientation of PCC in relation to the NE-striking σ_{Hmax}, defining a compressive domain that promotes stagnation, storage and differentiation of magmas (López-Escobar et al., 1995; Lara et al., 2006b; Cembrano and Lara, 2009). The apparent contradiction in extensional deformation along planes that are perpendicular to regional σ_{Hmax} has been explained in terms of the Andean earthquake deformation cycle (Sepúlveda et al., 2005). Extension is induced by co- and post-seismic relaxation, while compression dominates during inter-seismic periods. In fact, episodes of shallow extension have been observed after giant earthquakes and before/after eruptions (Jay et al., 2014). However, transpression is the dominant state of stress in the crust (Lavenu and Cembrano, 1999).

3. Methodology

3.1. Spatial distribution analyses

The CLV minor eruptive centers catalogue was created using published data (Moreno, 1977; Campos et al., 1998; Rodríguez, 1999), Google Earth imagery and field work. The result is a list of 65 MECs and one stratovolcano (in the Appendix), which was used to study the spatial distribution of vents.

Two types of spatial distribution analysis were performed: (1) volcanic alignments within CLV were determined using the *continuous sector* method, which is implemented in the 'Paleontological Statistics' software (PAST) (Hammer et al., 2001; Hammer, 2009). The radius *r* (which sets the length of the alignments to be detected), was set between 500 and 1500 m, in 100 m increments, using the range of maximum length alignments proposed by Le Corvec et al. (2013b). The significance level of the alignments was set to 90% in PAST; (2) spatial density estimates were performed using the kernel density estimation, with elliptical and circular Gaussian kernel functions (Connor et al., 2012). Elliptical kernel has the advantage of being potentially sensitive to tectonic controls on volcanism, although it creates a bias in the result (Kiyosugi et al., 2010). Circular kernel density estimate was performed to have an unbiased result to compare with. For details about the Kernel density estimation method, we refer the reader to the ample literature on density estimation (*e.g.* Martin et al., 2003; Connor et al., 2012).

3.2. Petrographic and geochemical analyses

We collected 30 CLV lava and scoria samples. Petrographic description was made using polarized microscopy and SEM. Major, minor and trace analyses were performed by ICP-MS and ICP-ES at ACME laboratories in Canada. Mineral chemistry analyses were conducted at the Geochemistry Laboratory of the Geology and Mining National Survey of Chile using SEM (ZEISS EVO MA-10, EDS Oxford X-AXT detector). Two Sr and Nd isotope ratios were determined with a mass spectrometer at Université Blaise Pascal in France, and we included twelve Sr and Nd isotope ratios from Sun (2001) and Rodríguez (1999). The PCC chemical data used for comparison was obtained from Singer et al. (2008) and references therein.

3.3. Volume estimation

The volume of CLV was estimated by measuring the volume enclosed between the topography and a subjacent surface. Völker et al. (2011) used this method considering flat basal planes, but, as they recognized, this method overestimates the volume in cases where volcanic products rest upon mountainous terrain. Using flat basal planes to estimate the volume in CLV would trap large portions of basement. For this reason, we modified this method in order to use it in CLV, considering that volcanic products are distributed in relatively thin sheets that cover the pre-existing rugged, glacial-eroded basement topography. The procedure is as follows: the area was divided in several tiles (Fig. 3), whose vertexes were set to the level of lakes, rivers or low-lying areas, generating a basal surface that conserves the general dip of the basement. The level of vertexes in rivers and low-lying areas was decreased by 10 m to include buried volcanic products. The thickness of basal lavas was estimated to be 40 m. Both values were estimated from exposures in rivers. Next, the volume was calculated using Global Mapper 14 software and Aster GDEM v.2 (downloaded from the Japan Space Systems website), with a vertical accuracy of 18.5 m (Gesch et al., 2011). To quantify the error induced by the DEM, two additional volume estimates were performed with tile vertexes lowered by 20 m and 0 m (50 m and 30 m for basal lavas), obtaining maximum and minimum volume estimates. Due to the limitations of this method (DEM resolution, thickness assumptions) a coarse estimation of CLV volume will be obtained, which is, however, enough for the purpose of this article.

3.4. Magma reservoir formation model

Several numerical models focus on the thermal structure needed to construct an upper crustal magma reservoir fed by sills and dikes (*e.g.* Annen and Sparks, 2002; Annen, 2009; Menand et al., 2011;

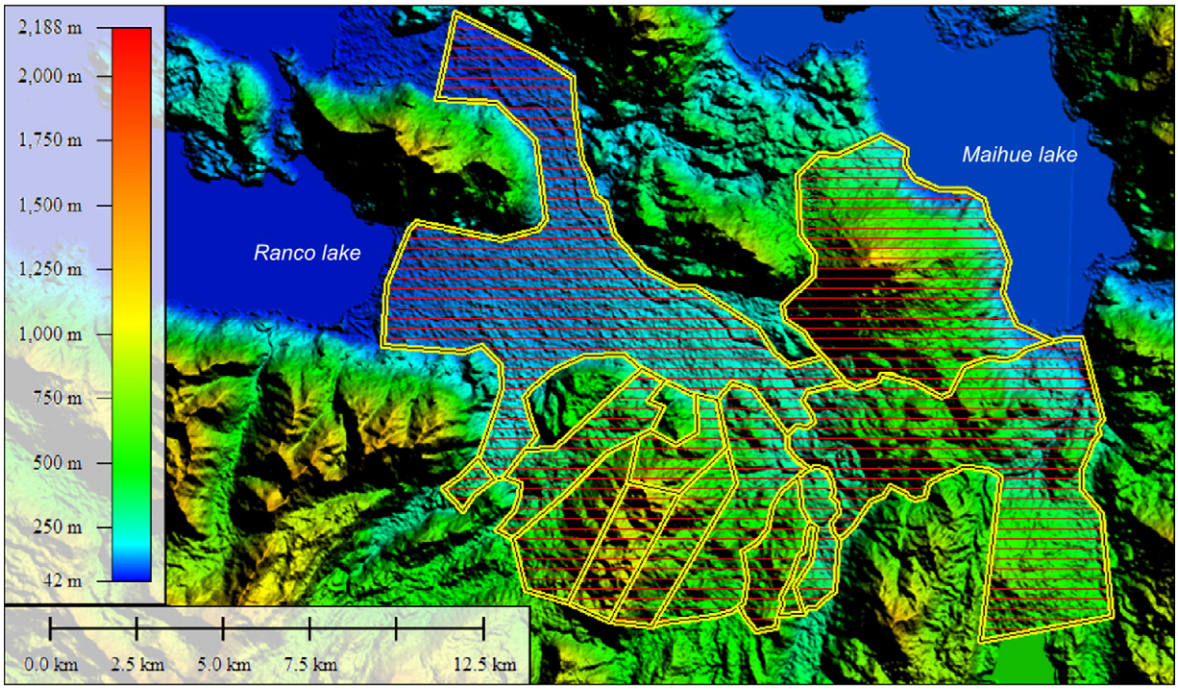

Fig. 3. Tiles used to estimate the volume of CLV.

Annen et al., 2013; Gelman et al., 2013; Menand et al., 2015; Molina et al., 2015). To evaluate the effect of magma flux on the construction of an upper-crustal magma reservoir, we used the results of the simulations performed by Gelman et al. (2013). This model was selected because it can also be used to evaluate the effect of basaltic and silicic compositions. We considered the physical parameters defined by Gelman et al. (2013), as we lacked specific geometric data on the PCC magma reservoir.

The Gelman et al. (2013) model determines the amount of eruptible magma available inside plutons that grow by vertical stacking of sills. These sills were assigned a thickness of 200 m and a diameter of 20 km each, and intrude the upper crust at depths between 5 and 15 km. The frequency of sill injection depends on the magma input rate (in km^3/ky). Other important parameters in this simulation are the geotherm (set to 30 °C/km), the T-dependant thermal conductivity (K) and the type of crystallization–temperature relationship (Gelman et al., 2013).

The main uncertainty in the use of this model is the magma flux (or magma input rate), which is unknown, hard to constrain, and in most cases can only be inferred from magma output rate. To account for this uncertainty, we considered a range of intrusive to extrusive (I:E) ratios obtained from literature (White et al., 2006), and discuss the implications of adopting different I:E ratios. Indeed, the results of this model are primarily dependant on magma flux and to a lesser extent on reservoir shape (Annen, 2009). As there is no geometrical data on the PCC reservoir(s), we decided to use this model's original parameters in order to have a first-order idea about the effect of different magma fluxes and compositions on the characteristics of the CLV and PCC volcanic systems.

4. Results: Spatial statistical analyses, petrography, geochemistry and time–volume relationships

4.1. Spatial statistical analyses

Volcanic alignments reflect the orientation and position of feeder dikes in monogenetic volcanic fields (Nakamura, 1977). In CLV, we found one preferred and two secondary orientations of volcanic alignments (Fig. 4a). The preferred orientation trends N40–60°E, similar to σ_{Hmax}, while the secondary orientations are N50°W and N10°E, matching the strike of the Futrono Fault and the LOFZ, respectively.

Spatial density estimation (Fig. 4b and c) using circular and elliptical kernels indicates that most MECs fall within a N65°E-trending corridor. Only the peripheral centers depart from this corridor. Two zones having a high density of vents ($>16\times10^{-3}$ vents/km^2) can be recognized within this corridor: one in the SW (Los Venados MECs) and another in the NE (Carrán MECs). Both zones are separated by the projected main trace of the LOFZ.

4.2. Petrographic and chemical characterization of CLV

In this section, the peripheral centers are described and plotted independently from the rest of CLV. Published data on PCC was plotted along with CLV data for ease of comparison (Singer et al., 2008). Results of the chemical analyses are presented in the Appendix.

CLV rocks are olivine–plagioclase phyric basalts and basaltic andesites (Fig. 5a). Mineral assemblage includes calcic-plagioclase, olivine, and (occasionally) clinopyroxene microphenocrysts (<2 mm), in a groundmass of plagioclase, clinopyroxene, olivine and Fe–Ti oxide microlites, and minor glass. Microphenocrysts of olivine show a reabsorption texture with a corona of orthopyroxene. Peripheral centers (Fig. 5b) are exclusively olivine–plagioclase phyric basalts. Olivines show no signs of reabsorption and are associated with chrome–spinel in a groundmass of plagioclase, olivine, clinopyroxene, and Fe–Ti-oxide microlites. Clinopyroxene shows a skeletal texture, which indicates high undercooling rates.

CLV magma composition ranges from non-primitive basalts to andesitic basalts (up to 56% SiO_2) (Fig. 6). All samples are low to medium-K and plot in the sub-alkaline field (Fig. 7a). They have low #Mg (<53) and low contents of Cr (<62 ppm) and Ni (<37 ppm). Peripheral centers show higher MgO (6.8%–7.7%) and CaO (8.4%–9.0%) and lower FeO_t (8.8%–9.4%) than the other CLV rocks. These centers have the highest #Mg (up to 61), Cr (130–198 ppm) and Ni (65–98 ppm) contents, being the most primitive CLV magmas.

In CLV and peripheral centers, Ni and Co show an inverse relationship with the degree of differentiation, suggesting olivine and Fe–Ti-

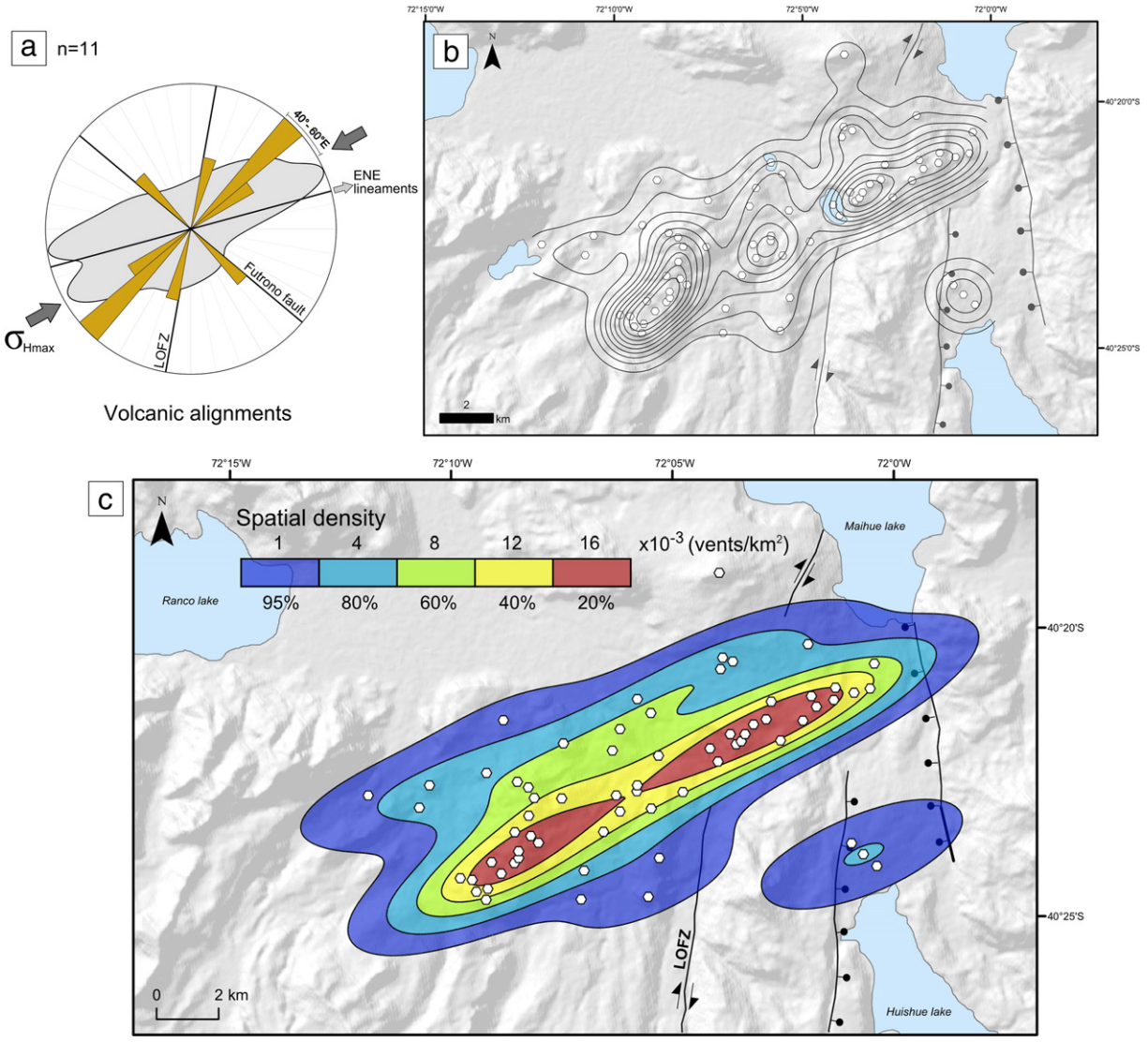

Fig. 4. (a) Volcanic alignment results, where one preferred orientation (N40°–60°E) and two secondary orientations (N10°E and N50°W) are recognized. CLV shape is shown in gray. (b) Vent density map with contours obtained using circular kernel analysis. (c) Vent density map obtained using elliptical kernel analysis, using circular. 95% of the MECs are located in a N65°E-striking corridor. Four centers are outside this corridor, namely, Los Guindos and Medialuna centers.

oxides fractionation, while clinopyroxene fractionation is inferred from depleted contents of Sc (<37 ppm) and V (<294 ppm). The N-MORB-normalized REE graph (Fig. 7b) shows a pattern typical of the CSVZ magmas, with complete overlap of CLV and PCC magmas. The HREE values suggest that garnet is absent in the source, and the peripheral centers show higher La/Yb ratios. All the products show the Nb and Ta troughs in the multielements diagram (Fig. 2 in the Appendix), characteristic of subduction-related magmatism. Finally, all CLV samples have

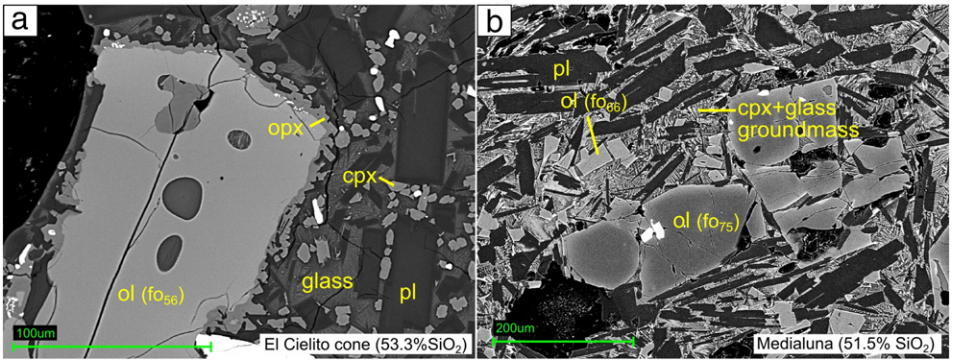

Fig. 5. SEM backscatter images of CLV rocks. (a) Basaltic andesite with microphenocryst of olivine, showing reabsorption texture and a corona of orthopyroxene. (b) Basalt from the Medialuna cones (peripheral centers) with microphenocrysts of olivine, and groundmass with clinopyroxene and glass. Clinopyroxene shows skeletal texture, evidencing a high undercooling.

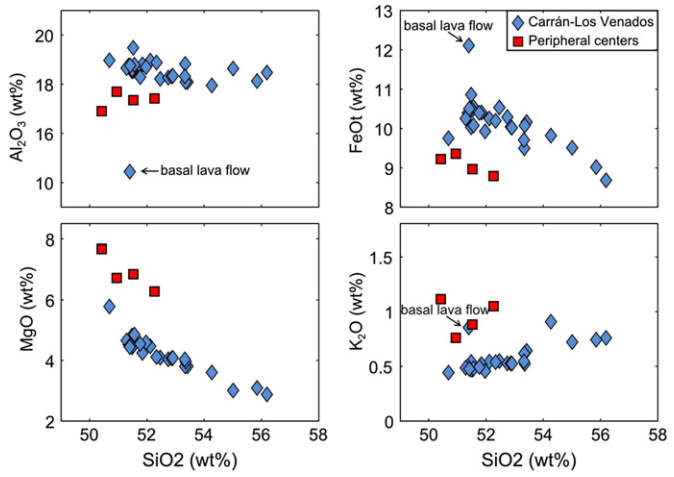

Fig. 6. Harker diagrams of CLV samples. Peripheral centers show a higher MgO and K_2O content, and lower FeO_t than the other CLV rocks. CLV Samples range from basalts to basaltic andesites, while peripheral centers have emitted only basalts.

$^{87}Sr/^{86}Sr$ ratios between 0.70401 and 0.70415, similar to those of PCC basalts and basaltic andesites (between 0.70378 and 0.70417) (Singer et al., 2008).

The isotopic and geochemical similarities between CLV and PCC basalts and basaltic andesites suggest similar source and differentiation processes. REE and trace element patterns are characteristic of an asthenospheric mantle source, with plagioclase or spinel as the aluminous phase melted due to hydration of the mantle wedge by slab fluids during subduction (Hildreth and Moorbath, 1988; Wagner et al., 2006; Gimenez et al., 2009). In addition, almost constant parallel REE patterns suggest that fractional crystallization is the most important differentiation process in CLV magmas, as proposed for PCC basalts and basaltic andesites (Lara et al., 2006b; Jicha et al., 2007; Singer et al., 2008). Other processes, like assimilation of the gabbroic lower crust, have been suggested to explain non-mantelic $^{87}Sr/^{86}$ Sr ratios of PCC magmas (Jicha et al., 2007), and could occur on CLV magma evolution magmas as well.

Petrographic and chemical characteristics of CLV are consistent with a magmatic evolution marked by deep crustal stagnation and differentiation, followed by rapid ascent to the surface. Stagnation in the lower crust would induce crystallization of Mg-rich olivine, plagioclase and Fe–Ti-oxides, which would be partly or totally fractionated. After this, syn-eruptive crystallization (during ascent or surface cooling) would generate clinopyroxene, olivine, plagioclase and Fe–Ti-oxide microlites in the groundmass. Within CLV, peripheral centers have erupted the most primitive magmas, which indicates that differentiation processes only proceeded to a lesser extent, which can be interpreted as lower residence times in deep crustal reservoirs, while the skeletal texture indicates a faster ascent compared to the rest of CLV.

4.3. Time–volume relationships

The estimated CLV volume is 14.4 ± 1.4 km^3, with Los Guindos contributing 45% of this value (6.2 ± 0.2 km^3). Post-glacial CLV volume was estimated to be 8.5 ± 1.2 km^3, with basal lavas accounting for 25% (2.1 ± 0.5 km^3). To our knowledge, the only previous estimate of CLV volume was 61 km^3 (Völker et al., 2011), which we consider unrealistic for a volcanic field with a relatively low number of MECs. For example, the Auckland Volcanic Field has an estimated volume of 3.4 km^3 (DRE) with *ca.* 50 vents (Allen and Smith, 1994). The probable reason for this overestimated value is that Völker et al. (2011) measured the volume enclosed between a flat basal plane at the elevation of Ranco Lake and the topography, trapping large portions of basement between those surfaces. CLV time–volume relationships are summarized in Table 2.

Magma flux values are needed to use the results of Gelman et al.'s (2013) numerical simulations. As magma flux is unknown, it is generally estimated based on magma output rate (Takada, 1994; White et al., 2006). This carries with it a considerable degree of uncertainty derived from the time–volume relationship estimation and the selected intrusive to extrusive (I:E) ratio. White et al. (2006) proposed 5:1 as a reasonable I:E ratio. Here, we use a range of I:E ratios from 4:1 to 6:1 to account for the above uncertainty. Thus, CLV magma flux is 2.4 ± 0.7 km^3/ky for the complete CLV, and 3.1 ± 1.0 km^3/ky for post-glacial CLV (Table 2). As for PCC, the estimated average magma flux is 2.1 ± 0.4 km^3/ky, which is lower than that of CLV. However, during PCC peak volcanism periods beginning at 124, 69 and 19 ka, the PCC magma flux (up to 5.5 ± 1.1 km^3/ky) was almost twice the CLV magma flux. These values are plotted in Fig. 8.

We distinguish here between two types of upper-crustal reservoirs: (1) stable reservoirs, which are permanent in time, permit differentiation of magma and contain eruptible magma. These reservoirs are characteristic of polygenetic systems; and (2) mush-type reservoirs, which are also permanent in time and permit differentiation, but lack eruptible magma because they are formed by a highly crystalline mush (following the criteria of Annen, 2009, based on Michaut and Jaupart, 2006). These reservoirs do not have superficial expression and cool over time forming plutons, unless magma flux increases sufficiently to heat the system and generate eruptible magma (Gelman et al., 2013), or unless silicic melts segregate from the crystalline mush to form shallower reservoirs (Dufek and Bachmann, 2010).

According to Gelman et al.'s (2013) results, basaltic magma accumulates in mush-type upper-crustal reservoirs only if it is injected at rates

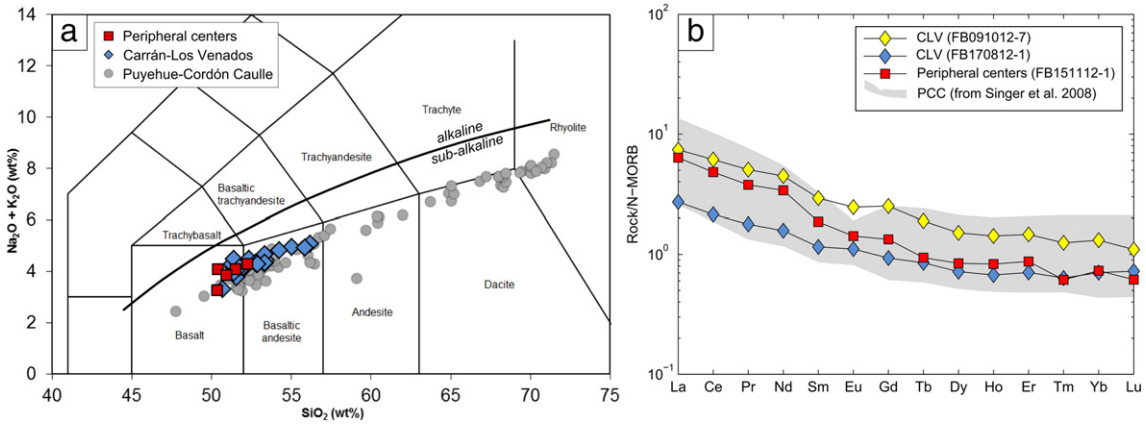

Fig. 7. (a) TAS diagram (Le Bas et al. 1986). CLV rocks plot in the sub-alkaline field, and overlap PCC rocks. (b) N-MORB-normalized REE plot. Peripheral centers have a higher La/Yb ratio compared to the other CLV samples. HREE values indicate absence of garnet in the source. CLV and PCC overlap completely. PCC data are from Singer et al. (2008).

Table 2
CLV time–volume relationships. CLV and PCC average output rates are similar, but PCC has had three peak output rate periods. We tabulate the first of these periods (*ca.* 124 to 96 ka). Magma flux is estimated using three different intrusion to extrusion (I:E) ratios.

Volcano	Volume (km3)	Age	Period of extrusion (ky)	Output rate (km3/ky)	Magma flux (I:E = 4:1)	Magma flux (I:E = 5:1)	Magma flux (I:E = 6:1)	Reference of output rate
Post-glacial CLV max	9.8	Post-glacial	13.9	0.71	2.8	3.5	4.2	This work
Post-glacial CLV best	8.5	Post-glacial	13.9	0.61	2.4	3.1	3.7	
Post-glacial CLV min	7.3	Post-glacial	13.9	0.53	2.1	2.6	3.2	
Complete CLV max	15.9	Mid-to-Late Pleistocene	30 (?)	0.53	2.1	2.7	3.2	
Complete CLV best	14.4	Mid-to-Late Pleistocene	30 (?)	0.48	1.9	2.4	2.9	
Complete CLV min	13.1	Mid-to-Late Pleistocene	30 (?)	0.44	1.7	2.2	2.6	
PCC peak 1	33	Medium Pleistocene	*ca.* 124 to 96 ka	1.1	4.4	5.5	6.6	Singer et al. (2008)
Complete PCC	131	Medium Pleistocene	314	0.42	1.7	2.1	2.5	

which exceed a certain threshold (long-dashed line in Fig. 9a). Besides, for this basaltic magma to be eruptible (stable reservoir), a greater magma flux is required (short-dashed line in Fig. 9a). According to this model, magma composition is a determining factor for reservoir evolution, because silicic reservoirs require lower magma flux to accumulate eruptible melt than basaltic reservoirs (dotted-dashed lines in Fig. 9a). Similarly, at a fixed input rate, the amount of eruptible magma is several times higher in a silicic reservoir than in a basaltic reservoir (Gelman et al., 2013).

Based on these numerical simulations, the estimated average CLV magma flux is in a limit situation, where the lower-range magma flux is not sufficient to build and maintain a 20-km diameter cylindrical upper-crustal reservoir, but the upper-range magma flux is enough to build a mush-type reservoir (Fig. 9a). In this analysis we considered the post-glacial CLV magma flux (3.1 ± 1.0 km^3/ky) because of the better temporal constrain of this value. As for PCC, the magma flux during periods of peak volcanism would have been sufficient (regardless I:E ratio) to produce and maintain a stable 20-km diameter upper-crustal reservoir containing ~10 km^3 of silicic eruptible magma (Fig. 9b). These results are discussed below.

5. Discussion

Our results show important differences between the Carrán–Los Venados and Puyehue–Cordón Caulle volcanic systems in terms of magmatic evolution, local crustal deformation and pattern of magma ascent. Below, we discuss how these differences can account for the contrasting styles of volcanism in CLV and PCC.

5.1. Petrogenesis and deep crustal processes

Petrographic and geochemical similarities between CLV and PCC basalts – *e.g.* $^{87}Sr/^{86}$ Sr ratios, HREE values and petrographic textures – are such that they cannot be distinguished. This suggests that both volcanic systems share the same upper-mantle and/or lower-crustal zones where initial differentiation processes occur. Hence, the difference in style of volcanism might result from differences in the upper-crustal components of the volcanic system.

As stated previously for CLV, the presence of only one group of high-pressure minerals in a groundmass of syn-eruptive crystals indicates a stage of deep crustal stagnation and differentiation (mainly fractional crystallization of olivine, clinopyroxene and Fe–Ti-oxides), and a subsequent rapid ascent to the surface. We found no evidence for the existence of a stable upper-crustal reservoir associated with CLV, which is in agreement with previous studies (López-Escobar et al., 1995; Lara et al., 2006a). In contrast, PCC has a broader compositional range, including dacites and rhyolites, which has been explained by low pressure fractional crystallization (Lara et al., 2006b; Singer et al., 2008). Therefore, compositional differences between CLV and PCC imply different crustal stagnation depths: while the CLV volcanic system includes only deep crustal reservoirs, the PCC volcanic system would also include one or several stable upper-crustal reservoirs (Lara et al., 2006b; Jay et al., 2014). This crucial element of polygenetic volcanic systems

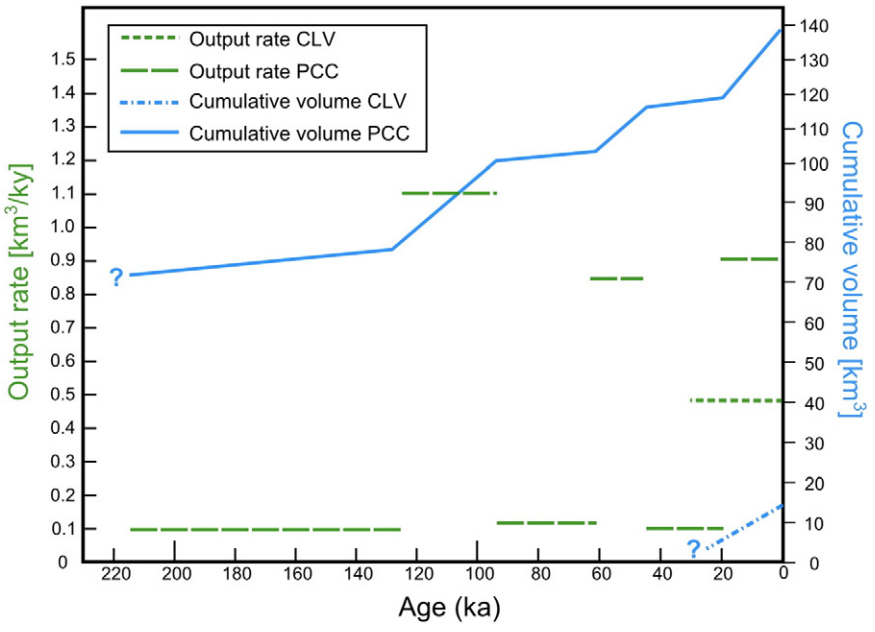

Fig. 8. CLV and PCC time–volume relationships. Note the three periods of high magma flux at PCC. PCC data are from Singer at al. (2008).

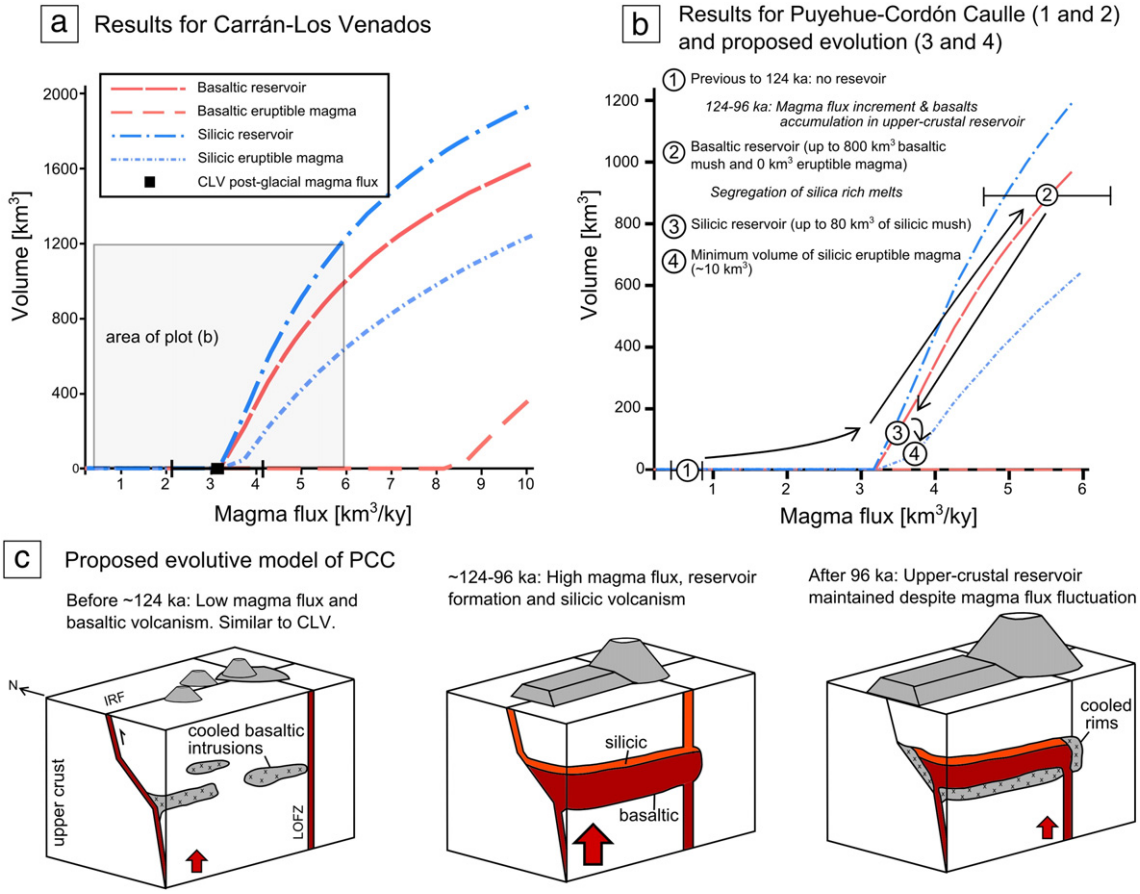

Fig. 9. (a) Volume of magma in reservoir and eruptible magma as a function of magma flux for 20-km diameter basaltic and silicic reservoirs (Gelman et al., 2013). CLV magma flux is in a limit situation regarding reservoir formation. (b) PCC estimated magma flux plotted on numerical simulation results. Numbers indicate the proposed sequence of PCC reservoir formation. (c) Drawings of proposed PCC upper-crustal reservoir evolution. IRF = Iculpe River Fault. See text for details.

promotes magma differentiation and favors the creation of a permanent conduit for magma extrusion due to continued feeding of new magmas (Takada, 1994; Cañón-Tapia and Walker, 2004; Németh, 2010; Kereszturi and Németh, 2012).

5.2. Upper-crustal magma reservoir formation

In order to envisage possible future scenarios for CLV, first we discuss the results obtained for PCC. PCC experienced multiple episodes wherein output rates peaked at values nearly an order of magnitude larger than the periods in between. Previous to *ca.* 133 ka, only basalts and basaltic andesites were emitted (<57% SiO_2). Then came an increase in silica content at *ca.* 133 ka (61.5% SiO_2), and magma output rate peaked between 124 and 96 ka, accompanied by extrusion of andesites and dacites (Singer et al., 2008).

Based on the Gelman et al. (2013) simulations, the 5.5 ± 1.1 km^3/ky peak magma flux at 124–96 ka (Table 2) was sufficient to create a mush-type basaltic reservoir containing 0% eruptible magma (Fig. 9b). However, the high-SiO_2 products erupted between 124 and 96 ka evidence differentiation of magma in upper-crustal reservoirs. This suggests that segregation of differentiated residual liquids in the mush-type reservoir occurred. This segregation is promoted in highly crystalline reservoirs (60–70 vol. %) with silicic melts tending to accumulate in the roof of the reservoir or in shallower reservoirs (Fig. 9c) (Dufek and Bachmann, 2010). Based on geochemistry and using MELTS, we estimate the silicic melts to be 10% of the reservoir created between 124 and 96 ka (Fig. 9b). As explained before, a silicic reservoir can sustain high-volume volcanism as a result of the greater amounts of eruptible magma compared with basaltic magma at the same temperature (Gelman et al., 2013). Singer et al. (2008) see a relationship between peak output rate in PCC and deglaciations. We suggest that ice retreat probably had a trigger effect on greater magma extrusion, but is not the causative factor behind the emission of silica-enriched magmas. In conclusion, we postulate that the peak of magmatism at 124–96 ka marks the beginning of polygenetic volcanism at PCC as it exists today, and that magma flux is a first-order factor that determines the style of volcanism.

For CLV, the estimated magma flux is in a limit situation, in which the I:E ratio is the main factor determining the result (Fig. 9a). While the lower-range estimated magma flux (I:E = 4:1) is not sufficient to build and maintain a 20-km diameter upper-crustal reservoir, the upper-range magma flux (I:E = 1:6) permits the formation of a basaltic mush-type reservoir that lacks eruptible magma (Fig. 9a).

Our chemical and petrographic evidence supports the absence of a stable upper-crustal magma reservoir associated with CLV, and this is consistent with the results obtained for the lower-range estimated magma flux. In this scenario, ephemeral minor upper-crustal reservoirs can form, as have been proposed for other monogenetic volcanoes (*e.g.* Johnson et al., 2008). They can account for the more evolved CLV magmas (up to 56% SiO_2) and do not survive after an eruptive event.

In the upper-range estimated magma flux, a mush-type reservoir with 0% eruptible magma could form under CLV, as the one created under PCC during peak magma flux. However, unlike PCC, there is no evidence for the segregation of silicic melts in the reservoir. The products erupted at CLV have been basaltic and basaltic andesitic, as occurred in PCC previous to the period of peak magma flux. We interpret this situation as CLV being at an inflection point, with magma flux as the determining factor. An increase of this parameter would shift the

equilibrium in favor of silicic melt segregation at the reservoir leading to polygenetic volcanism over time (López-Escobar and Moreno, 1994; Cañón-Tapia and Walker, 2004). Otherwise, this reservoir will cool to form a pluton and the system will remain monogenetic.

It is worth noting that CLV and PCC average magma flux have similar values (Table 2), although both have different styles of volcanism. It is the high PCC magma flux during certain periods that makes the difference for style of volcanism (Fig. 10).

5.3. Local crustal deformation and its influence on magma reservoir formation

The shape of volcanic fields has been associated to source and tectonic controls (Spörli and Eastwood, 1997; Cembrano and Lara, 2009). Applied to the CLV case, the source hypothesis would indicate that the CLV magma source is elongated in the NE direction. However, this hypothesis has been proved for intraplate systems with essentially isotropic stress fields (*e.g.* Spörli and Eastwood, 1997; Tadini et al., 2014). In tectonically active arc domains, with anisotropic stress fields and active basement faults, the tectonic hypothesis accounts for the good matching between the orientation of the CLV volcanic field (N65°E) and the σ_{Hmax} (N60°E). According to this hypothesis, the anisotropic stress field determines the geometry of the CLV plumbing system through the emplacement of dikes in a NE-striking extensional or transtensional crustal domain (López-Escobar et al., 1995; Cembrano and Lara, 2009), which is consistent with the observation that monogenetic volcanism is favored in extensional domains (Nakamura, 1977; Takada, 1994; Piochi et al., 2005). For PCC NW-striking volcanic system, this hypothesis implies that the system undergoes compressive deformation, except in the co-eruptive stages when localized extension has been observed (Jay et al., 2014).

These different deformation regimes could play an important role in the formation of upper-crustal reservoirs in CLV and PCC. In CLV, extension would promote magma ascent and subsequent extrusion instead of accumulation in the crust (*i.e.* lower I:E ratio) (Cañón-Tapia and Walker, 2004; Cembrano and Lara, 2009; Tibaldi et al., 2010), thereby setting CLV magma flux lower within the range of the estimated values (<3.5 km^3/ky). This condition hampers the formation of a stable reservoir, favoring rapid magma rise and the occurrence of persistent monogenetic volcanism. On the other hand, compression enhances the ability of PCC to accumulate magmas (*i.e.* higher I:E ratio) and create a stable upper-crustal reservoir. In this case study, local deformation promotes sustained monogenetic volcanism in CLV, diminishing its potential to evolve toward a polygenetic system.

CLV vent alignments suggest an interplay between structural and magmatic controls for magma ascent. Any of three alternatives is possible for feeder dikes: a) they are created parallel to NE-striking σ_{Hmax}, b) they use pre-existing fractures that are prone to open, or c) they change their trajectory when passing in between two pre-existing fractures, being channelized between them (Le Corvec et al., 2013a). In low magma pressure scenarios, NE-striking dikes are favored and NE-striking fractures or NNE-striking LOFZ faults influence dike orientation through one of the three above mechanisms. In light of the small-volume magma batches emitted at CLV, this scenario is to be expected under average conditions. However, changes of the stress regime may occur, for example during co- and post-seismic relaxation or during high magma pressure events, and NW-striking dikes could be favored (Roman et al., 2004; Cembrano and Lara, 2009; Le Corvec et al., 2013a).

6. Conclusions

We performed studies on CLV volcanic system and made comparisons with PCC in order to find the factors that would explain coeval and nearby sustained monogenetic and polygenetic volcanism in Southern Andes.

- The CLV volcanic system is characterized by an asthenospheric mantle source and deep crustal processes of differentiation, mainly fractioning of olivine, clinopyroxene and Fe–Ti-oxides, although assimilation of gabbroic lower crust may also occur. Some differentiation may also occur *en route* to the surface. CLV geochemical characteristics are similar to those of PCC mafic products.
- The good matching between the orientation of the CLV volcanic field (N65°E) and the σ_{Hmax} (N60°E) suggests dike emplacement in a NE-striking extensional or tenstensional crustal domain.
- CLV is in a limit situation regarding stable upper-crustal reservoir formation. With magma flux in the lower-range values, CLV magmas reach the surface directly from the lower crust or stagnate in ephemeral upper-crustal reservoirs. This scenario is favored by the local extensional or transtensional regime (lower I:E ratio). With magma flux in the upper-range values, mush-type reservoirs containing 0% eruptible magma are formed. If segregation of silicic melts occurs at this reservoir, the system will evolve toward polygenetic. Otherwise, the system will remain monogenetic. An increase in magma flux would shift the equilibrium in favor of polygenetic volcanism.

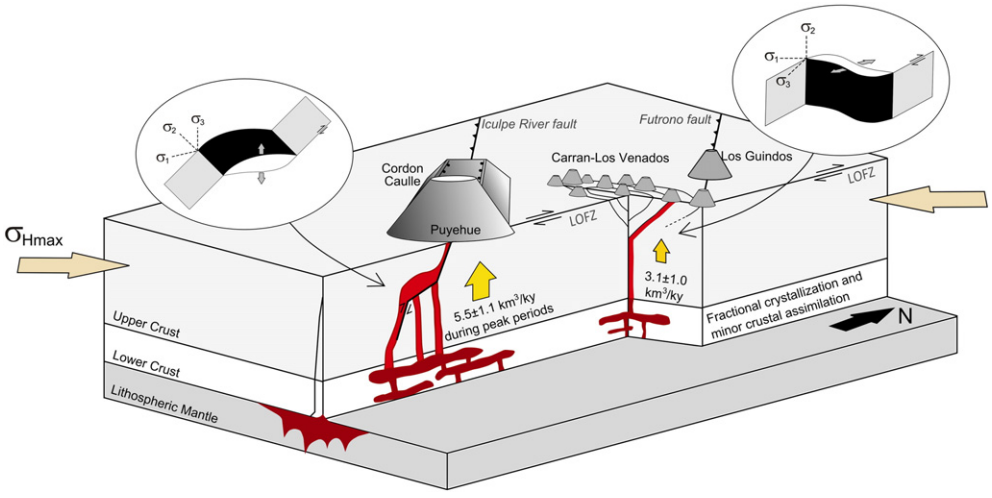

Fig. 10. Diagram depicting the main results of this study. Style of volcanism at CLV and PCC would be determined by the absence/presence of a stable upper-crustal reservoir. Upper-crustal reservoir formation is hampered at CLV by an insufficient magma flux and extensional or transtensional deformation of the crust. A mush-type upper-crustal reservoir can exist under CLV. Monogenetic volcanism will be maintained at CLV unless there is an increment of magma flux. Reworked Fig. 7 of Cembrano and Lara (2009).

Basaltic and basaltic andesitic magmas erupted at CLV suggest that segregation of silicic melts has not occurred below CLV.

- In PCC, a stable upper-crustal reservoir with silicic eruptible melt formed during the period of peak magma flux between 124 and 96 ka, favored by the local compressive deformation, and marks the beginning of polygenetic volcanism at PCC. The upper-crustal reservoir at PCC led to magmas with evolved compositions and to the creation of permanent conduits for magma extrusion.
- Different magma flux and local crustal deformation are the main factors that explain contrasting coeval and nearby styles of volcanism, in agreement with the pioneer model of Takada (1994).

Acknowledgments

Fieldwork and geochemistry was supported by Sernageomin and Fondecyt grant Nono. 11070222. J. Reyes and E. Morgado are thanked for their collaboration to this article's results. N. Le Corvec and A. Tibaldi are thanked for their very useful comments, which greatly improved this article. G. Bucchi is kindly thanked for his revision of the English. This is a contribution to the Volcano Hazards Program at Sernageomin, Chile. This article is dedicated to the mother of Francisco Bucchi.

Appendix A. Supplementary data

Supplementary data associated with this article can be found in the online version, at http://dx.doi.org/10.1016/j.jvolgeores.2015.10.013. These data include Google map of the most important areas described in this article.

References

Allen, S.R., Smith, I.E.M., 1994. Eruption styles and volcanic hazard in the Auckland volcanic field, New Zealand. Geosci. Rep. Shizuoka Univ. 20, 5–14.
Angermann, D., Klotz, J., Reigber, Ch., 1999. Space-geodetic estimation of the Nazca–South America Euler vector. Earth Planet. Sci. Lett. 171 (3), 329–334.
Annen, C., 2009. From plutons to magma chambers: thermal constraints on the accumulation of eruptible silicic magma in the upper crust. Earth Planet. Sci. Lett. 284 (3–4), 409–416.
Annen, C., Sparks, R.S.J., 2002. Effects of repetitive emplacement of basaltic intrusions on thermal evolution and melt generation in the crust. Earth Planet. Sci. Lett. 203 (3–4), 937–955.
Annen, C., Paulatto, M., Sparks, R.S.J., Minshull, T.A., Kiddle, E.J., 2013. Quantification of the intrusive magma fluxes during magma chamber growth at Soufrière Hills Volcano (Montserrat, Lesser Antilles). J. Petrol. http://dx.doi.org/10.1093/petrology/egt075.
Barrientos, S., Acevedo, P., 1992. Seismological aspects of the 1988–1989 Lonquimay (Chile) volcanic eruption. J. Volcanol. Geotherm. Res. 53, 73–87.
Brenna, M., Cronin, S.J., Smith, I.E.M., Sohn, Y.K., Németh, K., 2010. Mechanisms driving polymagmatic activity at a monogenetic volcano, Udo, Jeju Island, South Korea. Contrib. Mineral. Petrol. 160 (6), 931–950.
Campos, A., Moreno, H., Muñoz, J., Antinao, J.L., Clayton, K., Martin, M., 1998. Área Futrono-Lago Ranco, región de Los Lagos. Servicio Nacional de Geología y Minería, Mapas Geológicos No.8, escala 1:1000000. Santiago.
Cañón-Tapia, E., Walker, G.P.L., 2004. Global aspects of volcanism: the perspectives of "plate tectonics" and "volcanic systems". Earth Sci. Rev. 66, 163–182.
Cembrano, J., Lara, L., 2009. The link between volcanism and tectonics in the southern volcanic zone of the Chilean Andes: a review. Tectonophysics 471, 96–113.
Cembrano, J., Hervé, F., Lavenu, A., 1996. The Liquiñe–Ofqui fault zone: a long-lived intra-arc fault zone in southern Chile. Tectonophysics 259, 55–66.
Condit, C.D., Connor, C.B., 1996. Recurrence rates of volcanism in basaltic volcanic fields: an example from the Springerville volcanic field, Arizona. Geol. Soc. Am. Bull. 108 (10), 1225–1241. http://dx.doi.org/10.1130/0016-7606(1996)108<1225:rrovib>2.3.co;2.
Connor, C.B., Stamatakos, J.A., Ferrill, D.A., Hill, B.E., Ofoegbu, G.I., Conway, F.M., Sagar, B., Trapp, J., 2000. Geologic factors controlling patterns of small-volume basaltic volcanism: application to a volcanic hazards assessment at Yucca Mountain, Nevada. J. Geophys. Res. 105, 417–432.
Connor, L.J., Connor, C.B., Meliksetian, K., Savov, I., 2012. Probabilistic approach to modeling lava flow inundation: a lava flow hazard assessment for a nuclear facility in Armenia. J. Appl. Volcanol. 1, 1–19.
Dufek, J., Bachmann, O., 2010. Quantum magmatism: magmatic compositional gaps generated by melt-crystal dynamics. Geology 38, 687–690.
Fedotov, S.A., 1981. Magma rates in feeding conduits of different volcanic centres. J. Volcanol. Geotherm. Res. 9, 379–394.
Gelman, S.E., Gutiérrez, F.J., Bachmann, O., 2013. The longevity of large upper crustal silicic magma reservoirs. Geology 41, 759–762.
Gesch, D., Oimoen, M., Zhang, Z., Danielson, J., Meyer, D., 2011. Validation of the ASTER Global Digital Elevation Model (GDEM) Version 2 over the conterminous United States. Report to the ASTER GDEM Version 2.
Gimenez, M.E., Braitenberg, C., Martinez, M.P., Introcaso, A., 2009. A comparative analysis of seismological and gravimetric crustal thicknesses below the Andean Region with flat subduction of the Nazca Plate. Int. J. Geophys. 2009, 1–9. http://dx.doi.org/10.1155/2009/607458.
Glodny, J., Gräfe, K., Echtler, H., Rosenau, M., 2008. Mesozoic to quaternary continental margin dynamics in South–Central Chile (36°–42°S): the apatite and zircon fission track perspective. Int. J. Earth Sci. 97, 1271–1291.
Guzmán, P., 2013. Control tectónico de la evolución del paisaje cuaternario en la cuenca de intra-arco del lago Maihue, Andes del Sur. Región de Los Ríos, Chile. Universidad de Concepción, thesis (unpublished). 144 pp. Concepción, Chile.
Hammer, Ø., 2009. New statistical methods for detecting point alignments. Comput. Geosci. 35, 659–666.
Hammer, Ø., Harper, D.A.T., Ryan, P.D., 2001. PAST: Paleontological Statistics software package for education and data analysis. Palaeontol. Electron. 4 (1) (9 pp.).
Hildreth, W., 1981. Gradients in silicic magma chambers: implications for lithospheric magmatism. J. Geophys. Res. 86, 10153–10192.
Hildreth, W.S., Moorbath, S., 1988. Crustal contributions to arc magmatism in the Andes of Central Chile. Contrib. Mineral. Petrol. 98, 455–499.
Jay, J.A., Costa, F., Pritchard, M.E., Lara, L.E., Singer, B., Herrin, J., 2014. Locating magma reservoirs using InSAR and petrology before and during the 2011–2012 Cordón Caulle silicic eruption. Earth Planet. Sci. Lett. 295, 254–266.
Jicha, B.R., Singer, B.S., Beard, B.L., Johnson, C.M., Moreno, H., Naranjo, J.A., 2007. Rapid magma ascent and generation of 230 Th excesses in the lower crust at Puyehue–Cordón Caulle, southern volcanic zone, Chile. Earth Planet. Sci. Lett. 255 (1–2), 229–242.
Johnson, E.R., Wallace, P.J., Cashman, K.V., Granados, H.D., Kent, A.J.R., 2008. Magmatic volatile contents and degassing-induced crystallization at Volcán Jorullo, Mexico: implications for melt evolution and the plumbing systems of monogenetic volcanoes. Earth Planet. Sci. Lett. 269, 478–487. http://dx.doi.org/10.1016/j.epsl.2008.03.004.
Kereszturi, G., Németh, K., 2012. Monogenetic basaltic volcanoes: genetic classification, growth, geomorphology and degradation. In: Németh, K. (Ed.), Updates in volcanology — new advances in understanding volcanic systems. InTech http://dx.doi.org/10.5772/51387.
Kiyosugi, K., Connor, C.B., Zhao, D., Connor, L.J., Tanaka, K., 2010. Relationships between volcano distribution, crustal structure, and P-wave tomography: an example from the Abu mono-genetic volcano group, SW Japan. Bull. Volcanol. 72, 331–340. http://dx.doi.org/10.1007/s00445-009-0316-4.
Lange, D., Cembrano, J., Rietbrock, A., Haberland, C., Dahm, T., Bataille, K., 2008. First seismic record for intra-arc strike-slip tectonics along the Liquiñe–Ofqui fault zone at the obliquely convergent plate margin of the southern Andes. Tectonophysics 455, 14–24.
Lara, L.E., Naranjo, J.A., Moreno, H., 2004. Rhyodacitic fissure eruption in southern Andes (Cordón Caulle; 40.5°S) after the 1960 (Mw: 9.5) Chilean earthquake: a structural interpretation. J. Volcanol. Geotherm. Res. 138, 127–138.
Lara, L.E., Lavenu, A., Cembrano, J., Rodríguez, C., 2006a. Structural controls of volcanism in transversal chains: resheared faults and neotectonics in the Cordón Caulle–Puyehue area (40.5°S), southern Andes. J. Volcanol. Geotherm. Res. 158, 70–86. http://dx.doi.org/10.1016/j.jvolgeores.2006.04.017.
Lara, L.E., Moreno, H., Naranjo, J.A., Matthews, S., Pérez de Arce, C., 2006b. Magmatic evolution of the Puyehue–Cordón Caulle volcanic complex (40°S), southern Andean volcanic zone: from shield to unusual rhyolitic fissure volcanism. J. Volcanol. Geotherm. Res. 157, 343–366. http://dx.doi.org/10.1016/j. jvolgeores.2006.04.010.
Lavenu, A., Cembrano, J., 1999. Compressional and transpressional-stress pattern for Pliocene and Quaternary brittle deformation in fore arc and intra-arc zones (Andes of Central and southern Chile). J. Struct. Geol. 21, 1669–1691.
Le Corvec, N., Menand, T., Lindsay, J., 2013a. Interaction of ascending magma with pre-existing crustal fractures in monogenetic basaltic volcanism: an experimental approach. J. Geophys. Res. 118 (3), 968–984. http://dx.doi.org/10.1002/jgrb.50142.
Le Corvec, N., Spörli, K.B., Rowland, J., Lindsay, J., 2013b. Spatial distribution and alignments of volcanic centers: clues to the formation of monogenetic volcanic fields. Earth Sci. Rev. 124, 96–114. http://dx.doi.org/10.1016/j.earscirev.2013.05.005.
López-Escobar, L., Moreno, H., 1981. Erupción de 1979 del volcán Mirador, Andes del Sur, 40°21'S: características geoquímicas de las lavas y xenolitos graníticos. Rev. Geol. Chile 13–14, 17–33.
López-Escobar, L., Moreno, H., 1994. Geochemical characteristics of the southern Andes basaltic volcanism associated with the Liquiñe–Ofqui fault zone between 39° and 46°S. Congreso Geologico Chileno, 7° vol. II, pp. 1388–1393.
López-Escobar, L., Cembrano, J., Moreno, H., 1995. Geochemistry and tectonics of the Chilean southern Andes basaltic quaternary volcanism (37–46°S). Rev. Geol. Chile 22 (2), 219–234.
Martin, A.J., Takahashi, M., Umeda, K., Yusa, Y., 2003. Probabilistic methods for estimating the long-term spatial characteristics of monogenetic volcanoes in Japan. Acta Geophys. Pol. 51, 271–291.
Menand, T., de Saint-Blanquat, M., Annen, C., 2011. Emplacement of magma pulses and growth of magma bodies. Tectonophysics 500 (1–4), 1–2. http://dx.doi.org/10.1016/j.tecto.2010.05.014.
Menand, T., Annen, C., de Saint Blanquat, M., 2015. Rates of magma transfer in the crust: insights into magma reservoir recharge and pluton growth. Geology 43, 199–202. http://dx.doi.org/10.1130/g36224.1.
Michaut, C., Jaupart, C., 2006. Ultra-rapid formation of large volumes of evolved magma. Earth Planet. Sci. Lett. 250 (1–2), 38–52.
Molina, P.G., Parada, M.A., Gutiérrez, F.J., Ma, C., Li, J., Yuanyuan, L., Reich, M., Aravena, A., 2015. Protracted late magmatic stage of the Caleu pluton (central Chile) as a consequence of heat redistribution by diking: insights from zircon data and thermal modeling. Lithos 227, 255–268.

Moreno, H., 1977. Geología del área volcánica Puyehue–Carrán en los Andes del sur de Chile. Universidad de Chile, thesis (unpublished). 181 pp. Santiago.
Nakamura, K., 1977. Volcanoes as possible indicators of tectonic stress orientation: principle and proposal. J. Volcanol. Geotherm. Res. 2, 1–16.
Németh, K., 2010. Monogenetic volcanic fields: origin, sedimentary record, and relationship with polygenetic volcanism. In: Cañón-Tapia, E., Szakács, A. (Eds.), What is a volcano? Geological Society of America Special Paper 470, pp. 43–66. http://dx.doi.org/10.1130/2010.2470(04).
Piochi, M., Bruno, P.P., De Astis, G., 2005. Relative roles of rifting tectonics and magma ascent processes: inferences from geophysical, structural, volcanological, and geochemical data for the Neapolitan volcanic region (southern Italy). Geochem. Geophys. Geosyst. 6, Q07005. http://dx.doi.org/10.1029/2004GC000885.
Rodríguez, C., 1999. Geoquímica del Grupo Carrán–Los Venados, Andes del Sur (40.3°S). Universidad de Chile, thesis (unpublished). 133 pp. Santiago.
Roman, D.C., Moran, S.C., Power, J.A., Cashman, K.V., 2004. Temporal and spatial variation of local stress fields before and after the 1992 eruptions of Crater Peak Vent, Mount Spurr Volcano, Alaska. Bull. Seismol. Soc. Am. 94 (6), 2366–2379. http://dx.doi.org/10.1785/0120030259.
Rosenau, M., Melnick, D., Echtler, H., 2006. Kinematic constraints on intra-arc shear and strain partitioning in the southern Andes between 38°S and 42°S latitude. Tectonics 25, TC4013.
Runge, M., Bebbington, M., Cronin, S., Lindsay, J., Kenedi, C., Moufti, M., 2014. Vents to events: determining an eruption event record from volcanic vent structures for the Harrat Rahat, Saudi Arabia. Bull Volcanol 76 (3), 1–16. http://dx.doi.org/10.1007/s00445-014-0804-z.
Sepúlveda, F., Lahsen, A., Bonavalot, S., Cembrano, J., Alvarado, A., Letelier, P., 2005. Morphostructural evolution of the Cordón–Caulle geothermal region, southern volcanic zone, Chile: insights from gravity and 40Ar/39Ar dating. J. Volcanol. Geotherm. Res. 148, 165–189. http://dx.doi.org/10.1016/j.jvolgeores.2005.03.020.
Singer, B.S., Jicha, B.R., Naranjo, J.A., Lara, L.E., Moreno, H., Harper, M., 2008. Eruptive history, geochronology, and magmatic evolution of the Puyehue–Cordón Caulle volcanic complex, Chile. Geol. Soc. Am. Bull. 120, 599–618.
Spörli, B.K., Eastwood, V.R., 1997. Elliptical boundary of an intraplate volcanic field, Auckland, New Zealand. J. Volcanol. Geotherm. Res. 79 (3–4), 169–179.
Straub, S.M., Gomez-Tuena, A., Stuart, F.M., Zellmer, G.F., Espinasa-Perena, R., Cai, Y., Iizuka, Y., 2011. Formation of hybrid arc andesites beneath thick continental crust. Earth Planet. Sci. Lett. 303 (3–4), 337–347. http://dx.doi.org/10.1016/j.epsl.2011.01.013.
Sun, M., 2001. Geochemical variation among small eruptive centers in the central SVZ of the Andes: an evaluation of subduction, mantle and crustal influences. ProQuest ETD Collection for FIU. Paper AAI3025237 (http://digitalcommons.fiu.edu/dissertations/AAI3025237).
Tadini, A., Bonali, F.L., Corazzato, C., Cortés, J.A., Tibaldi, A., Valentine, G.A., 2014. Spatial distribution and structural analysis of vents in the lunar crater volcanic field (Nevada, USA). Bull. Volcanol. 76 (11), 1–15.
Takada, A., 1994. The influence of regional stress and magmatic input on styles of monogenetic and polygenetic volcanism. J. Geophys. Res. 99, 13,563–13,573.
Tibaldi, A., 1995. Morphology of pyroclastic cones and tectonics. J. Geophys. Res. 100 (B12), 24521–24535.
Tibaldi, A., 2015. Structure of volcano plumbing systems: a review of multi-parametric effects. J. Volcanol. Geotherm. Res. 298, 85–135.
Tibaldi, A., Pasquarè, F., Tormey, D., 2010. Volcanism in reverse and strike-slip fault settings. In: Cloetingh, S., Negendank, J. (Eds.), New Frontiers in Integrated Solid Earth Sciences. Springer-Verlag, pp. 315–348.
Valentine, G.A., Perry, F.V., 2007. Tectonically controlled, time-predictable basaltic volcanism from a lithospheric mantle source (central basin and range province, USA). Earth Planet. Sci. Lett. 261, 201–216. http://dx.doi.org/10.1016/j.epsl.2007.06.029.
Völker, D., Kutterolf, S., Wehrmann, H., 2011. Comparative mass balance of volcanic edifices at the southern volcanic zone of the Andes between 33°S and 46°S. J. Volcanol. Geotherm. Res. 205, 114–129. http://dx.doi.org/10.1016/j.jvolgeores.2011.03.011.
Wagner, L.S., Beck, S., Zandt, G., Ducea, M.N., 2006. Depleted lithosphere, cold, trapped asthenosphere, and frozen melt puddles above the flat slab in central Chile and Argentina. Earth Planet. Sci. Lett. 245 (1), 289–301.
Walker, G.P.L., 1993. Basaltic-volcano systems. In: Prichard, H.M., Alabaster, T., Harris, N.B.W., Neary, C.R. (Eds.), Magmatic processes and plate tectonics. Spec. Publ.-Geol. Soc., pp. 3–38.
White, S.M., Crisp, J.A., Spera, F.J., 2006. Long-term volumetric eruption rates and magma budgets. Geochem. Geophys. Geosyst. 7, Q03010. http://dx.doi.org/10.1029/2005GC001002.